Available online at www.sciencedirect.com
ScienceDirect
Trans. Nonferrous Met. Soc. China 26(2016) 1555−1563
Transactions of Nonferrous Metals Society of China
www.tnmsc.cn

Microstructure and properties of Al/Cu bimetal in liquid−solid compound casting process

Yuan HU, Yi-qing CHEN, Li LI, Huan-dong HU, Zi-ang ZHU

School of Materials Science and Engineering, Hefei University of Technology, Hefei 230009, China

Received 3 June 2015; accepted 28 September 2015

Abstract: A Ni−P coating was deposited on Cu substrate by electroless plating and the Al/Cu bimetal was produced by solid−liquid compound casting technology. The microstructure, mechanical properties and conductivity of Al/Cu joints with different process parameters (bonding temperature and preheating time) were investigated. The results showed that intermetallics formed at the interface and the thickness and variety increased with the increase of bonding temperature and preheating time. The Ni−P interlayer functioned as a diffusion barrier and protective film which effectively reduced the formation of intermetallics. The shear strength and conductivity of Al/Cu bimetal were reduced by increasing the thickness of intermetallics. In particular, the detrimental effect of Al_2Cu phase was more obvious compared with the others. The sample preheated at 780 °C for 150 s exhibited the maximum shear strength and conductivity of 49.8 MPa and 5.29×10^5 S/cm, respectively.

Key words: Al/Cu bimetal; solid−liquid compound casting; electroless Ni plating; Al_2Cu phase; microstructure; mechanical properties; conductivity

1 Introduction

Bimetal compound materials have been widely studied and used in the last few decades attributing to its combination of the unique and numerous advantages of the bimetals，such as copper and aluminum compound structure [1−3]. Copper and its alloys have high electrical, thermal conductivity and low contact resistance. Aluminum and its alloys possess excellent properties such as low cost, high conductivity, high corrosion resistance and low density [4−6]. Therefore, there has been a growing interesting in joining Al and Cu together for playing the dual function of them. In fact, with extraordinary performances, they are widely used in electricity industries, acting as shield line, cable cleats and conductive strips [7−9].

There are many kinds of welding techniques such as cold roll welding [10,11], cold rolling [12], diffusion bonding [13,14], brazing [15,16], explosive welding [17,18], friction welding [19,20] and friction stir welding [21−23], which have been developed as alternative joining processes for joining Al and Cu. In these papers, particular difficulties of every method are introduced, but in summary, long process time, high processing cost and specific requirements for the shape of the substrate, may render these solid state joining processes as not easy for practical and industrial applications. Compound casting process is characterized as a process in which a metallic melt is cast onto or around a solid metal substrate, forming a liquid−solid diffusion reaction zone and thus a continuous metallic transition forms from one metal to the other. In the past three decades, the application of compound casting process was successfully applied in the field of bonding copper and aluminum because it can potentially provide an economical way to produce this bimetal without restriction of geometry and dimension [24−26].

In previous reports, we found some problems existing in Al/Cu couples, for example, ineffective surface treatment for copper, high temperature thermal oxidation and large amount of brittle intermetallic compounds at the interface of Al/Cu couple, such as Al_2Cu, AlCu, Al_2Cu_3, Al_3Cu_4 and Al_4Cu_9 [4,10,17,23,27]. Hence, a protective film on Cu substrate as well as a barrier preventing Al/Cu atom diffusion may be utility for Al/Cu couples. Recently, considerable theoretical and experimental studies have been carried out on diffusion

Foundation item: Project (51571080) supported by the National Natural Science Foundation of China
Corresponding author: Yi-qing CHEN; Tel: +86-551-62901139; E-mail: chenyq63@ hfut.edu.cn
DOI: 10.1016/S1003-6326(16)64261-9

bonding to study the effect of Ni interlayer, such as Mo/Cu [28], SS/Ti [29] and Mg/Al [30], and the results indicated that the Ni interlayer is helpful for improving the mechanical properties of dissimilar bimetals. ZHAO et al [8] have applied electroless Ni coating on Al in diffusion-bonded Al/Cu bimetal as Ni can substantially dissolve in Al and Cu, which makes it practical as an intermediate material. However, few researches have been conducted in compound casting process using electroless Ni coating on Cu substrate. Since electroless Ni coating on copper has shown great conveniences and advantages in previous works [31−34], it is worthy to investigate the feasibility and effect of the electroless Ni coating as an interlayer for Al/Cu bimetallic joint via compound casting process.

In this work, a Ni−P film with thickness of approximately 6 μm is deposited on the polished and cleaned Cu substrate, and the comparison of Al/Cu joints with and without Ni−P interlayer is made. Microstructural changes, relevant mechanical properties and conductivity are evaluated. The objective of the present research is to obtain Al/Cu bimetal with good performance by compound casting process.

2 Experimental

2.1 Materials and substrate preparation

The liquid−solid diffusion bonding was carried out on pure copper (T2) sheets and 6061 Al alloy plates with dimensions of 20 mm × 15 mm × 3 mm and 50 mm × 5 mm × 3 mm, respectively. The chemical compositions of the alloys are shown in Table 1.

Table 1 Chemical compositions of T2 Cu and 6061 Al alloys (mass fraction, %)

Alloy	Ag	Cu	Mn	Fe	Zn	Ni
Cu(T2)	0.05	Bal.	−	0.005	0.005	0.005
6061Al	−	0.15−0.4	0.15	0.7	0.25	−

Alloy	Pb	Mg	S	Si	Al
Cu(T2)	0.005	−	0.005	−	−
6061Al	−	0.8−1.2	−	0.4−0.8	Bal.

To get a compact coating and achieve a sound joint, some pre-treatments of the bimetallic samples are important. The essential steps are as follows. First of all, the samples were mechanically polished on 150 to 600 abrasive papers to offer clean and smooth surfaces; subsequently, they were ultrasonically cleaned in an acetone bath to remove adhered contaminants and then washed with alcohol and dried in air. Thereafter, Cu specimens were subjected to chemical cleaning which is an alkaline mixed solution comprising of sodium hydroxide and several sodium salts at 50−60 °C for 15 min to remove residual oils and fats adhering to the surface. Afterwards, as exposure to the air, there may be oxidation film on the cleaned Cu surface, and the acid pickling is necessary to gain an unoxidized surface. The unoxidized surface was obtained at room temperature for 30 s by dipping in a solution of 10% H_2SO_4 solution (volume fraction). The specimens must be rinsed with distilled water and dried in air after each chemical cleaning. Finally, after the wash-up in distilled water, the substrates were quickly transferred to the plating bath with constant temperature of 88 °C and pH value of 4.5 for 40 min. After the last step of surface pre-treatment, the immersion plating must be performed as soon as possible to avoid oxidation of the substrate. This procedure can ensure the direct contact between the coating layer and the substrate. The composition and condition of plating solution are given in Table 2.

Table 2 Plating solution for electroless nickel

Parameter	Value
Concentration of nickel sulfate/(g·L^{-1})	35
Concentration of sodium hypophosphite/(g·L^{-1})	40
Concentration of lactic acid/(mL·L^{-1})	20
Concentration of oxalic acid/(mg·L^{-1})	15
Concentration of propionic acid/(mL·L^{-1})	5
Concentration of sodium fluoride/(g·L^{-1})	0.5
Concentration of zinc nitrate/(mg·L^{-1})	4
Temperature/°C	88
pH	4.5

2.2 Experiments and analyses

Al/Cu compound casting process was performed in a self-designed tube furnace to investigate the interfacial bonding and reactions that occurred between molten aluminum and the copper substrate. The schematic of the device for bimetallic experiments and relative operations were introduced in our previous report [35].

The microstructure and bonding behavior at the interface of the Al/Cu bimetallic samples were examined using an optical microscope (MR2000), a scanning electron microscope (SIRION200), and an electron probe micro-analyzer (JXA−8230) equipped with energy dispersions spectroscopy. A mechanical testing machine (MTS809) was used to determine the shear strength of the Al/Cu samples. The setup used for determining the shear strength of the bimetallic samples was described by XU et al [35]. The average dimensions of the shear strength specimens were 15 mm × 15 mm × 6 mm.

A high precision micro-ohmmeter with accuracy of 0.01 Ω was used to measure the electrical resistance of Al/Cu bimetal samples. ABBASI et al [10] have explained the details of this test method. Here, a power

supply was used to create voltage between the surfaces of the bimetal and then the current created by this supply voltage between these two surfaces was measured. The potential difference between two different points of the sample with defined distance (L) can be measured when the micro-ohmmeter passes a certain current (I). Then, the microprocessor of the micro-ohmmeter calculated automatically the resistance (R) of the distance (L) of the bimetal according to the Ohm law ($R=U/I$). The mathematic equation was described below:

$$R=\frac{\Delta U}{I} \tag{1}$$

The necessary dimensions of the sample (width and thickness) were measured by a micrometer of 0.01 mm accuracy and then the resistivity (ρ) of the sample was calculated by the following equation:

$$\rho=\frac{RS}{L} \tag{2}$$

where S is the cross section area.

3 Results and discussion

3.1 Characterization of electroless Ni−P coating

Since standard oxidation−reduction potential of $H_2PO_2^-/HPO_3^{2-}$ couple (−1.57 V) is less than that of Ni^{2+}/Ni couple (−0.25 V) [32], the oxidation−reduction reaction can occur. The overall reaction is expressed by two equations:

$$H_2PO_2^-+H_2O+Ni^{2+}=3H^++HPO_3^{2-}+Ni \tag{3}$$

$$H_2PO_2^-+3H_{ad}=H_2O+OH^-+P+H_2\uparrow \tag{4}$$

The SEM images of Ni coating are shown in Fig. 1. It can be seen in Fig. 1(a) that a lubricious and uniform Ni coating with thicknesses of 6−8 μm was obtained on Cu substrates after 40 min deposition, which can be functioned as an interlayer between Cu substrate and molten Al in the compound casting. Figure 1(b) exhibits the Ni coating surface morphology featuring a compact cell-shaped structure corresponding to the white ellipsoidal particles. Figure 1(c) shows the distribution of major elements (Cu, Ni, P) along the black line from the Cu substrate to the coating surface marked in Fig. 1(a). The elemental compositions of the Ni coating are shown in Fig. 1(d). The EDS results of the analyzed zone marked in Fig. 1(b) reveal that the coating is Ni−P alloy with Ni content of 91.25% and P content of 8.63% (mass fraction). Here, P will deoxidate CuO with the formation of oxide ($2P+5CuO=5Cu+P_2O_5$). And then, this oxide will form a composite with the oxidation of copper. The composite was liquid spreading out on the surface of copper during the compound casting process, which was also helpful for removing oxides formed on Cu surface [36].

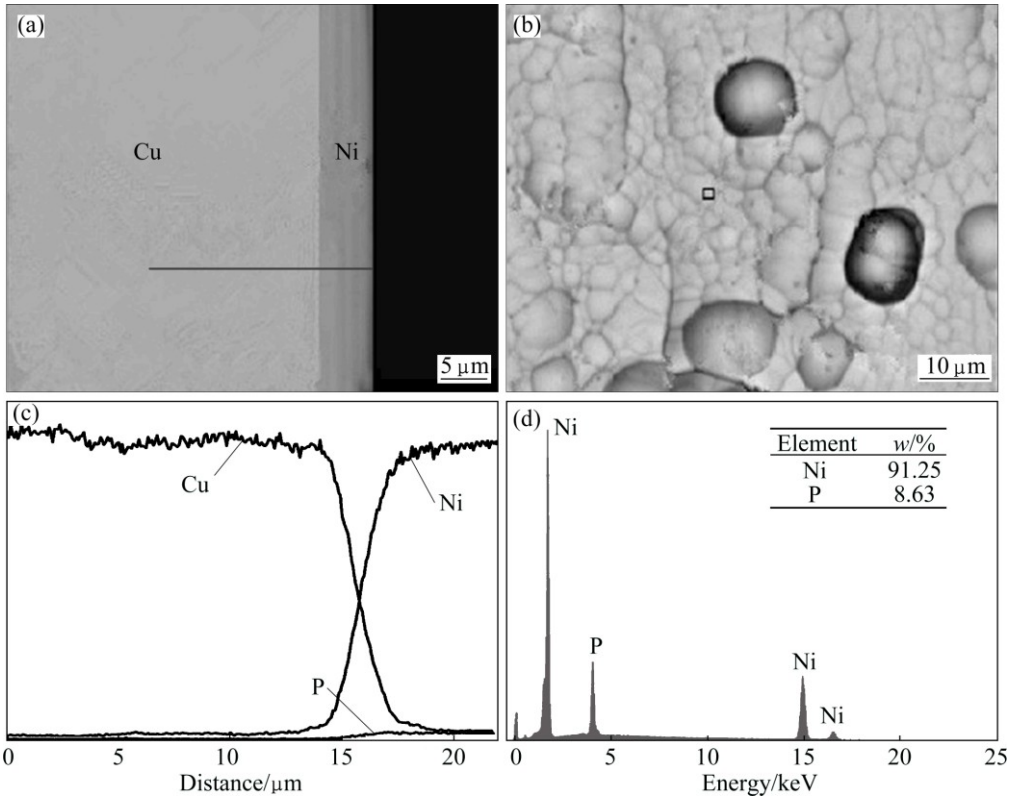

Fig. 1 SEM images of Ni−P coating on Cu substrate for 40 min: (a) Cross-section of Cu substrate; (b) Surface morphology; (c) Element distribution of major element (Cu, Ni, P); (d) EDS of Ni coating

3.2 Microstructure and formation mechanism

Figure 2(a) shows the microstructure of cross-section SEM image of the Al/Cu joint during the compound casting process with a bonding temperature of 800 °C and preheating time of 160 s (Sample 1). There are three different regions from Al matrix to Cu substrate, marked as I, II and III, which can be recognized as follows: eutectic+dendritic α(Al) structure, eutectic structure and intermetallic layers, respectively. Besides, there are obvious gaps at the interface, indicating that a perfect metallurgical bonding is not achieved. On the one hand, it is suggested that the oxides form rapidly on the surface during the experimental process of this work despite the mechanical and chemical pretreatment of Cu substrate. Consequently, the atom diffusion of the melt and the substrate is prevented. On the other hand, because the linear expansion coefficients of Al, Cu and intermetallics are different, the gap will be formed during cooling process. Finally, it results in local and limited metal bond. The higher magnification images of rectangles *A* and *B* marked in Fig. 2(a) are shown in Figs. 2(b) and (c), respectively. In Fig. 2(b), the magnification of the eutectic structure is exhibited. According to the Cu−Al binary phase diagram shown in Fig. 3, the dark area is α(Al), the scattered grey region is Al_2Cu (θ), the reaction can be described as $L \xrightarrow{548.2^{\circ}C} \alpha(Al)+\theta$. In Fig. 2(c), it can be seen that the grey Al_2Cu phases appear block mingled with trifling α(Al), which can be affirmed as hypereutectic structure by the Cu−Al binary phase diagram. In order to analyze the constitutive phases of region III close to the Cu substrate, the measurement of X-ray diffraction pattern was carried out. The results indicate that the light grey region with no obvious boundary is composed of AlCu and Al_4Cu_9 phases. The phases can be further affirmed by EPMA of four different positions (*P*1−*P*4 in Fig. 2(d)) that there are AlCu and Al_4Cu_9 Cu-rich phases from Al matrix to Cu, which is consistent with the previous studies [17,23,25]. The mole fractions of Cu and Al were measured and the results are demonstrated in Table 3.

Figure 4 shows the interfacial micrographs of Al/Cu sample (Sample 2) with Ni interlayer under the same condition as Sample 1. As seen in Fig. 4(a), the Al/Cu couple with Ni interlayer has a continuous metallurgical bonding without any cracks or gaps and also three diffusion regions appear except abundant Al_2Cu bulks produced by hypereutectic reaction. The higher magnification of rectangular *A* marked in Fig. 4(a) is shown in Fig. 4(b). The AlCu and Al_4Cu_9 phases still exist close to the Cu substrate just like that shown in Fig. 2(c), which can be affirmed by XRD pattern shown in Fig. 5(b). It can be seen in Fig. 4(b) that there are

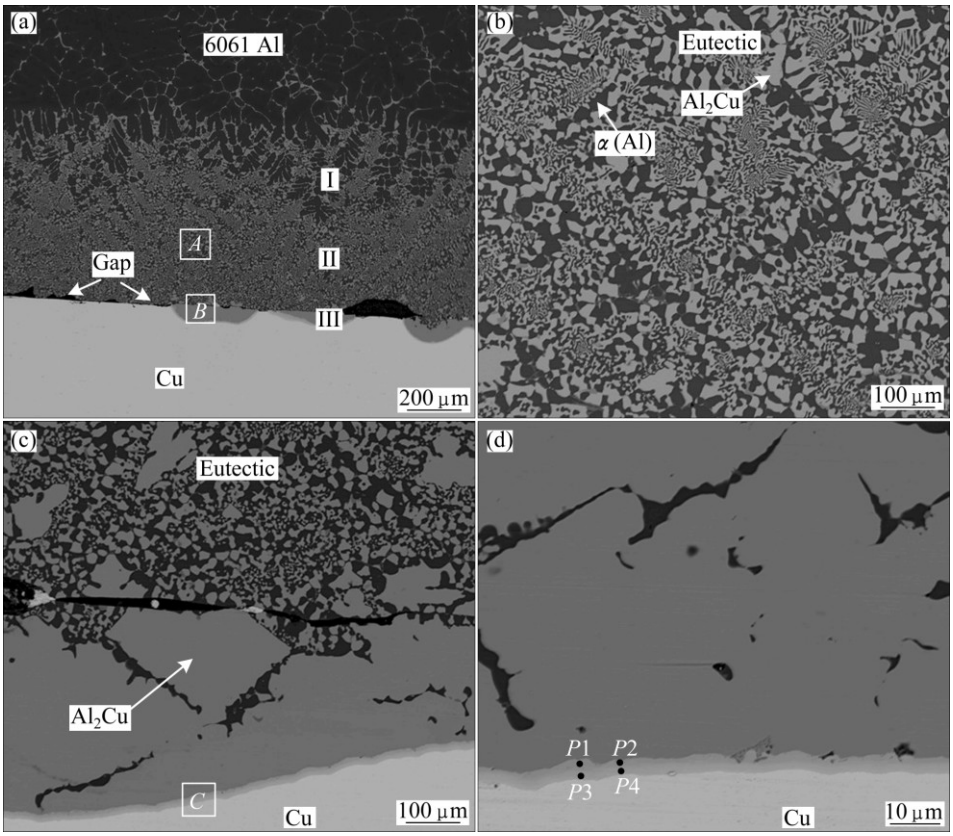

Fig. 2 SEM images of interfacial microstructure of Al/Cu joint direct bonding at 800 °C for 160 s (Sample 1): (a) Microstructure of cross-section; (b) Magnified image of rectangle *A* in (a); (c) Magnified image of rectangle *B* in (a); (d) Magnified image of rectangle *C* in (c)

Table 3 EPMA quantitative analysis results for points marked in Figs. 2(d), 4(b), 6(d) and 6(f)

Position	Mole fraction/%			Possible phase
	Al	Cu	Ni	
*P*1	50.1707	49.0890	−	AlCu
*P*2	49.9892	48.0807	−	
*P*3	29.1510	69.7384	−	Al_4Cu_9
*P*4	28.4647	70.5342	−	
*P*5	56.2887	41.6576	1.8115	$Al_{55.97}Cu_{41.69}Ni_{2.16}$
*P*6	55.6541	41.7303	2.5151	
*P*7	58.4721	39.4524	2.0654	$Al_{59.08}Cu_{39.23}Ni_{2.19}$
*P*8	59.6814	39.0094	2.3081	
*P*9	32.1624	67.8365	−	Al_4Cu_9
*P*10	29.8137	69.2872	−	
*P*11	39.8111	59.8789	−	Al_2Cu_3
*P*12	40.4550	59.3418	−	
*P*13	42.8421	57.1578	−	Al_3Cu_4
*P*14	41.9356	58.0643	−	
*P*15	49.5390	50.0774	−	AlCu
*P*16	50.3565	48.6434	−	

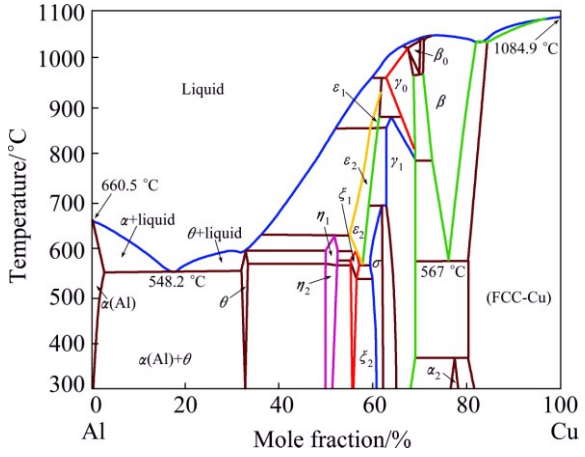

Fig. 3 Cu−Al binary phase diagram

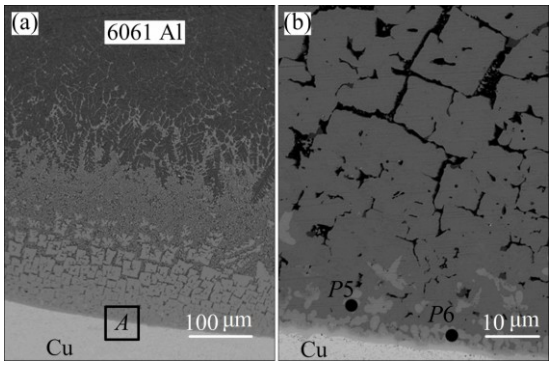

Fig. 4 SEM images of Al/Cu interface with Ni interlayer at 800 °C for 160 s (Sample 2): (a) Microstructure of cross-section; (b) Magnification of rectangle *A*

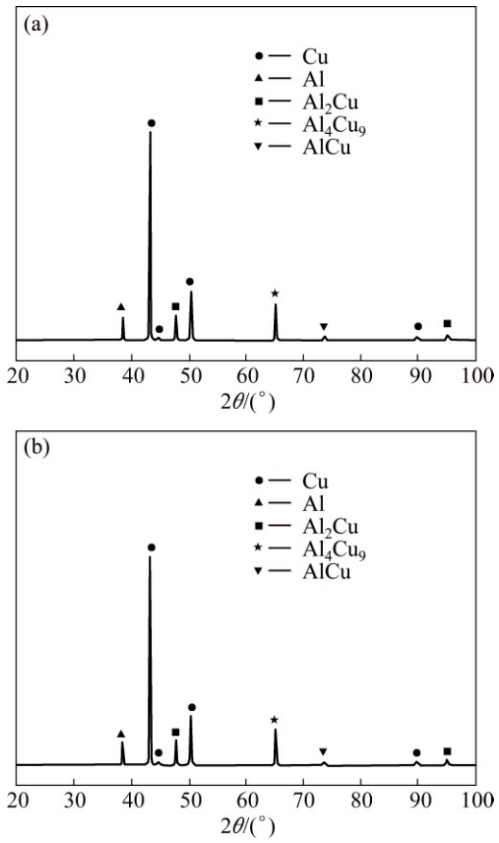

Fig. 5 XRD patterns of interface close to Cu side: (a) Sample 1; (b) Sample 2

many shallow blocks painted on the Al_2Cu phases. It can be analyzed by means of EPMA and the results shown in Table 3 indicate that the phase contains Ni. Its chemical composition is $Al_{55.97}Cu_{41.69}Ni_{2.16}$. However, there are no brittle Al−Ni intermetallic compounds. This may be ascribed to that the growth rate of Al−Cu intermetallics is much faster than that of Al−Ni intermetallics [8] and the thickness of Ni interlayer is not enough to react with Al.

Compared with the direct bonded Al/Cu specimen under the same experimental condition, the interfacial microstructure of Al/Cu specimen with Ni interlayer is improved obviously. It is suggested that Ni interlayer functioning as a protective film can inhibit oxides formation on Cu surface, helping form continuous metallic transition from liquid Al to solid Cu. The Ni interlayer solved the difficulty described in previous study [25].

In order to investigate the influences of bonding temperature and preheating time on the Al/Cu couple and find out the appropriate process parameters of compound casting process, further study on these two experimental parameters was carried out. The SEM images of the cross-section of Al/Cu joints obtained at 750 °C for 120 s (Sample 3), 780 °C for 150 s (Sample 4) and 820 °C for 180 s (Sample 5) are shown in Figs. 6(a), (c) and (e),

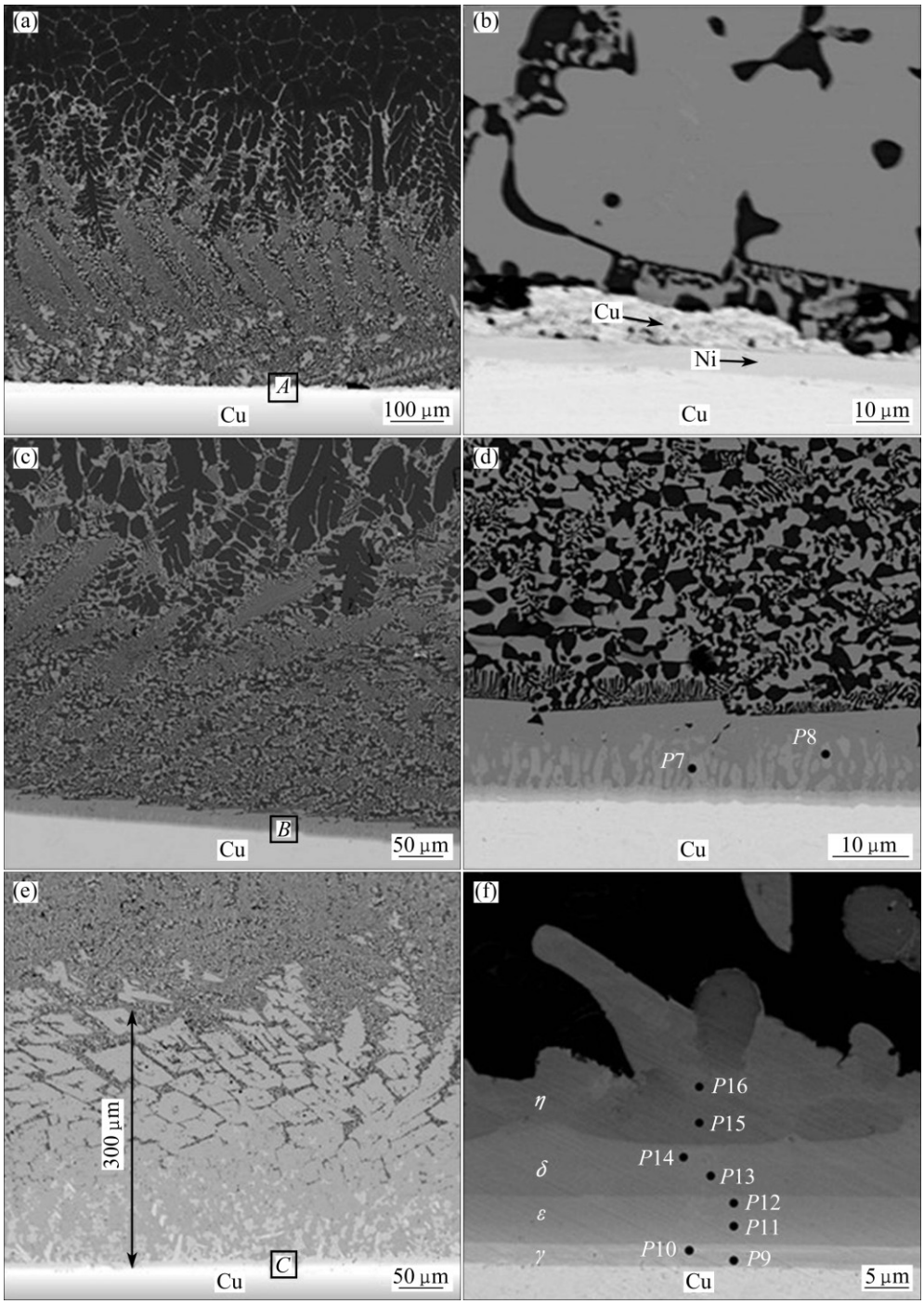

Fig. 6 SEM images of interface of Al/Cu bimetal with Ni interlayer at different temperatures and preheating time: (a) Sample 3 (750 °C, 120 s); (c) Sample 4 (780 °C, 150 s); (e) Sample 5 (820 °C, 180 s); (b, d, f) Magnified images of rectangles *A*−*C*, respectively

respectively. As seen in Fig. 6, we can draw the conclusion that the higher the bonding temperature is and the longer the preheating time is, the thicker and the more types of layers of Al/Cu intermetallics are formed. If the bonding temperature and preheating time are decreased, the diffusion of the atoms is limited inevitably and a metal bond cannot be achieved, which can be seen in Fig. 6(a). Al ingress through Ni interlayer into the Cu substrate is found to be highly dependent on the temperature and time, so there are no Cu-rich phases appearing at previous Al/Cu interface. It is suggested that the Ni interlayer impedes the Al atoms from diffusing into the Cu substrate completely. Nevertheless, the Cu atoms still pass across the Ni interlayer diffusing into Al melt in a way as there are Al_2Cu phases. The magnification of the rectangle *A* shown in Fig. 6(b)

proves that. It is because Cu atoms have the priority to diffuse to the Ni coating because of different diffusion coefficients of them [8]. In Fig. 6(c), the best Al/Cu joint is achieved under median bonding temperature and preheating time, in which intermetallic compounds are largely decreased from 300 to 25 μm compared with the joint shown in Fig. 6(e). The magnification images of rectangles *B* and *C*, marked in Figs. 6(c) and (e), are illustrated in Figs. 6(d) and (f), respectively. As seen in Fig. 6(d), there are $Al_{59.08}Cu_{39.23}Ni_{2.19}$ phases painted on Al_2Cu phase, which can be identified by EPMA. In addition, there are AlCu and Al_4Cu_9 layers directing to the Cu substrate based on the analysis above. Obviously, it can be noticed in Fig. 6(f) that the types of the layers are more and the width of each layer is much thicker than that of region at previous Al/Cu interfaces. There are four separated layers. In order to identify each layer, XRD analysis of interface close to Cu side is shown in Fig. 7. And chemical compositions of the positions labeled in Fig. 6(f) were measured by EPMA and the results are listed in Table 3. According to the XRD pattern as well as the results of EPMA and previous reports, each reaction layer from Al side to Cu side is corresponding to one of the Cu−Al intermetallic compounds AlCu (η), Cu_3Al_2 (δ), Cu_4Al_3 (ε), Al_4Cu_9 (γ), respectively [4,10,17].

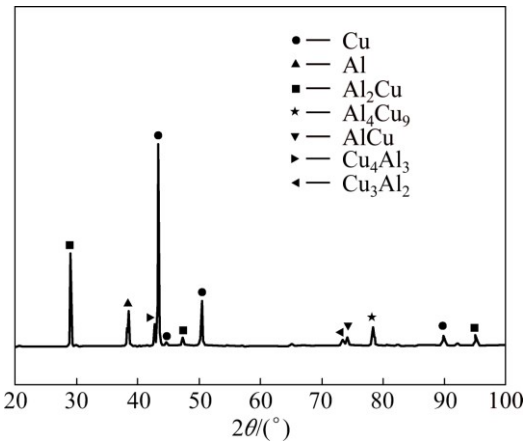

Fig. 7 XRD pattern of interface close to Cu side (Sample 5)

3.3 Interfacial strength of joint

The shear strength test was performed to evaluate the whole mechanical properties of the Al/Cu joints. Figure 8 illustrates the average values of the shear strength tests obtained under different bonding temperatures and preheating time with and without Ni interlayer. Sample 1 represents the sample without Ni interlayer, whereas Samples 2−5 represent those with Ni interlayer. We may make a conclusion from the shear strength tests results as follows. On the one hand, the joints cast with Ni interlayer have higher shear strength than that without Ni interlayer under the same experimental condition. On the other hand, the joints have a decrease in shear strength when cast at higher temperature and longer time. It can be convinced from the values that the Ni coating is useful for improving the mechanical properties. In addition, if a sound metallurgical joint is achieved via adjusting time and temperature of the compound process, a slight increase of shear strength will be obtained. When achieving a sound metallurgical bonding, the amount and thickness of the brittle intermetallics have a great effect on the mechanical properties. It can be seen that the highest shear strength is 49.8 MPa, indicating that less and thinner brittle intermetallic layers are favorable to the mechanical properties of the bimetal, which are corresponding to the processing parameters of 780 °C for 150 s.

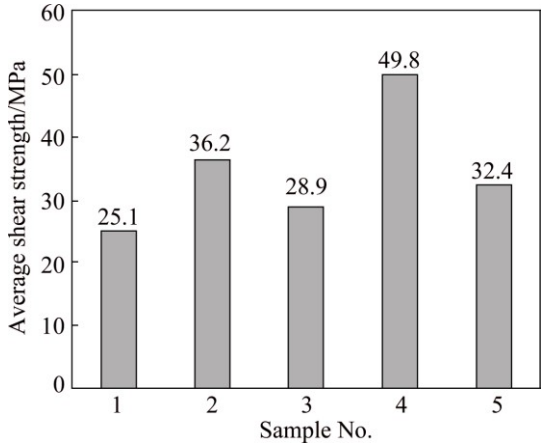

Fig. 8 Average shear strength of Al/Cu joints at different bonding temperature and preheating time: Sample 1 (800 °C, 160 s, without Ni); Sample 2 (800 °C, 160 s, with Ni); Sample 3 (750 °C, 120 s); Sample 4 (780 °C, 150 s); Sample 5 (820 °C, 180 s)

3.4 Conductivity

Electrical properties of the produced Al/Cu bimetal samples were evaluated by their resistivity. Table 4 illustrates the resistivity and conductivity of Al/Cu bimetal, measured by micro-ohmmeter and calculated in accordance with Eqs. (1) and (2). As can be known, Al/Cu bimetal has a median value between the resistivities of copper and aluminum. As ABBASI et al [10] reported that the resistance increased with increasing the intermetallic thickness due to the formation of low conductivity intermetallic layers. With increasing bonding temperature and preheating time, the thickness of intermetallics increases from 25 to 300 μm, the conductivity decreases from 5.29×10^5 to 3.83×10^5 S/cm. Of all the intermetallics, the detrimental effect of Al_2Cu phase is obvious because of the high proportion compared with the others. In addition, the laminar Al_2Cu phases of the eutectic structure formed dispersedly in different regions have no detrimental effect on the

electrical conductivity of the Al/Cu bimetal, while the Al_2Cu bulks of the hypereutectic structure with a high volume fraction damage the electrical conductivity badly.

Table 4 Resistivity and conductivity of Al, Cu and Al/Cu bimetal

Material	Resistivity/($\Omega\cdot mm^2\cdot m^{-1}$)	Conductivity/($S\cdot cm^{-1}$)
Al	2.84×10^{-2} (Ref. [2])	3.52×10^{5}
Cu	1.75×10^{-2} (Ref. [2])	5.71×10^{5}
Al/Cu	2.61×10^{-2}−1.89×10^{-2}	3.83×10^{5}−5.29×10^{5}

4 Conclusions

1) Liquid Al−solid Cu compound casting process was carried out on joining Al/Cu dissimilar metals using a Ni−P interlayer at different bonding temperatures and preheating time. The effects of Ni interlayer, bonding temperature and preheating time on the microstructure and properties of Al/Cu joints were investigated.

2) The electroless Ni−P coating as a protective film as well as a diffusion barrier can effectively inhibit the formation of oxides on the Cu substrate and help to develop a sound metallurgical bonding. Thus, in this work, the method about bonding Al/Cu bimetal via liquid−solid compound casting process is introduced and electroless Ni plating is feasible.

3) The high bonding temperature and long preheating time prompt the diffusion between the melt and solid and the formation of brittle intermetallic compounds. The maximum interfacial shear strength of the composites is obtained at 780 °C for 150 s.

4) The conductivity of Al/Cu bimetal decreases with the formation of intermetallic layers, especially the detrimental influence of Al_2Cu phase. However, the Al/Cu bimetal gets better electrical properties than the aluminum materials and combines the light mass advantage of aluminum.

References

[1] ACARER M. Electrical, corrosion, and mechanical properties of aluminum−copper joints produced by explosive welding [J]. Journal of Materials Engineering and Performance, 2012, 21(11): 2375−2379.

[2] ZHEN Yu, DUAN Yu-ping, LIU Li-dong, LIU Shun-hua, LIU Xu-jing, LI Xiao-gang. Growth behavior of Al/Cu intermetallic compounds in hot-dip aluminized copper [J]. Surface and Interface Analysis, 2009, 41(5): 361−365.

[3] LEE J E, BAE D H, CHUNG W S, KIM K H, LEE J H, CHO Y R. Effects of annealing on the mechanical and interface properties of stainless steel/aluminum/copper clad−metal sheets [J]. Journal of Materials Processing Technology, 2007, 187−188: 546−549.

[4] ZHAO Hong-jin, WANG Da, QIN Jing, ZHANG Ying-hui. Research progress on bonding mechanism and interface reaction of Al/Cu laminated composite [J]. Hot Working Technology, 2011, 40(10): 84−87.

[5] SASAKE T T, MORRIS R A, THOMPSON G B, SYARIF Y, FOX D. Formation of ultra-fine copper grains in copper-clad aluminum wire [J]. Scripta Materialia, 2010, 63(5): 488−491.

[6] WANG Juan, LI Ya-jiang, LIU Peng, GENG Hao-ran. Microstructure and XRD analysis in the interface zone of Mg/Al diffusion bonding [J]. Journal of Materials Processing Technology, 2008, 205(1−3): 146−150.

[7] RHEE K Y, HAN W Y, PARK H J, KIM S S. Fabrication of aluminum/copper clad composite using hot hydrostatic extrusion process and its material characteristics [J]. Materials Science and Engineering A, 2004, 384(1−2): 70−76.

[8] ZHAO Jia-lei, JIE Jin-chuan, CHEN Fei, CHEN Hang, LI Ting-ju, CAO Zhi-qiang. Effect of immersion Ni plating on interface microstructure and mechanical properties of Al/Cu bimetal [J]. Transactions of Nonferrous Metals Society of China, 2014, 24(6): 1659−1665.

[9] CHEN C Y, HWANG W S. Effect of annealing on the interfacial structure of aluminum−copper joints [J]. Materials Transactions, 48(7): 1938−1947.

[10] ABBASI M, TAHERI A K, SALEHI M T. Growth rate of intermetallic compounds in Al/Cu bimetal produced by cold roll welding process [J]. Journal of Alloys and Compounds, 2001, 319(1−2): 233−241.

[11] ABBASI M, SALEHI M T, TAHERI A K. An investigation on cold roll welding of copper to aluminum using electrical resistivity [J]. Zeitschrift fur Metallkunde, 2001, 92(5): 423−430.

[12] SHENG L Y, YANG F, XI T F, LAI C, YE H Q. Influence of heat treatment on interface of Al/Cu bimetal composite fabricated by cold rolling [J]. Composites: Part B, 2011, 42(6): 1468−1473.

[13] GUO Ya-jie, LIU Gui-wu, JIN Hai-yun, SHI Zhong-qi, QIAO Guan-jun. Intermetallic phase formation in diffusion-bonded Al/Cu laminates [J]. Journal of Materials Science, 2011, 46(8): 2467−2473.

[14] CALVO F A, URENG A, GOMEZ SALAZAR J M, MOLLEDA F. Special features of the formation of the diffusion bonded joints between copper and aluminium [J]. Journal of Materials Science, 1988, 23(6): 2273−2280.

[15] FENG Ji, XUE Song-bai, LOU Ji-yuan, LOU Yin-bin, WANG Shui-qing. Microstructure and properties of Al/Cu joints brazed with Zn−Al filler metals [J]. Transactions of Nonferrous Metals Society of China, 2012, 22(2): 281−287.

[16] JI Feng, XUE Song-bai, DAI Wei. Reliability studies of Al/Cu joints brazed with Zn−Al−Ce filler metals [J]. Materials & Design, 2012, 42: 156−163.

[17] HENRYK P, LIDIA L D, MARIUSZ P. Microstructure and phase constitution near the interface of explosively welded aluminum/ copper plates [J]. Metallurgical and Materials Transactions A, 2013, 44(8): 3836−3851.

[18] GULENC B. Investigation of interface properties and weldability of aluminum and copper plates by explosive welding method [J]. Materials & Design, 2008, 29(1): 275−278.

[19] ARITOSHI M, OKITA K, ENJO T, IKEUCHI K, MATSUDA F. Friction welding of oxygen free copper to pure aluminum [J]. Welding International, 1992, 6(11): 853−859.

[20] YILBAS B S, SAHIN A Z, KAHRAMAN N, AL-GARNI A Z. Friction welding of steel−Al and Al−Cu materials [J]. Journal of Materials Processing Technology, 1995, 49(3): 431−443.

[21] ZHANG Qiu-zheng, GONG Wen-biao, LIU Wei. Microstructure and mechanical properties of dissimilar Al−Cu joints by friction stir welding [J]. Transactions of Nonferrous Metals Society of China, 2015, 25(6): 1779−1786.

[22] XUE P, NI D R, WANG D, XIAO B L, MA Z Y. Effect of friction stir welding parameters on the microstructure and mechanical properties of the dissimilar Al−Cu joints [J]. Materials Science and Engineering A, 2011, 528: 4683−4689.

[23] SAEID T, ABDOLLAH-ZADEH A, SAZGARI B. Weldability and mechanical properties of dissimilar aluminum−copper lap joints made by friction stir welding [J]. Journal of Alloys and Compounds, 2010, 490(1−2): 652−655.
[24] PAPIS J M K, LOEFFLER J F, UGGOWITZER P J. Light metal compound casting [J]. Science in China Series E: Technological Sciences, 2009, 52(1): 46−51.
[25] ZARE G R, DIVANDARI M, ARABI H. Investigation on interface of Al/Cu couples in compound casting [J]. Materials Science and Technology, 2013, 29(2): 190−196.
[26] HAJJARI E, DIVANDARI M, RAZAVI S H, EMAMI S M, HOMMA T, KAMADO S. Dissimilar joining of Al/Mg light metals by compound casting process [J]. Journal of Materials Science, 2011, 46(20): 6491−6499.
[27] TANAKA Y, KAJIHARA M, WATANABE Y. Growth behavior of compound layers during reactive diffusion between solid Cu and liquid Al [J]. Materials Science and Engineering A, 2007, 445−446: 355−363.
[28] ZHANG Jian, XIAO Yuan, LUO Guo-qiang, SHEN Qiang, ZHANG Lian-meng. Effect of Ni interlayer on strength and microstructure of diffusion-bonded Mo/Cu joints [J]. Materials Letters, 2012, 66(1): 113−116.
[29] KUNDU S, CHATTERJEE S. Characterization of diffusion bonded joint between titanium and 304 stainless steel using a Ni interlayer [J]. Materials Characterization, 2008, 59(5): 631−637.
[30] ZHANG Jian, LUO Guo-qiang, WANG Yi-yu, XIAO Yuan, SHEN Qiang, ZHANG Lian-meng. Effect of Al thin film and Ni foil interlayer on diffusion bonded Mg−Al dissimilar joints [J]. Journal of Alloys and Compounds, 2013, 556(15): 139−142.
[31] MALECKIA A, MICEK-ILNICKA A. Electroless nickel plating from acid bath [J]. Surface and Coatings Technology, 2000, 123(1): 72−77.
[32] TANG Zuo-qin, HU Su-rong, CHAO Yin-chun. Electroless nickel plating on copper foil [J]. Advanced Materials Research, 2014, 926: 103−107.
[33] DAI K J, XIONG Y, YIN J H. Electroless Ni−P coating on Cu substrate with strike nickel activation and its corrosion resistance [J]. Materialwissenschaft und Werkstofftechnik, 2013, 44(11): 918−921.
[34] HO C E, FAN C W, HSIEH W Z. Pronounced effects of Ni(P) thickness on the interfacial reaction and high impact resistance of the solder/Au/Pd(P)/Ni(P)/Cu reactive system [J]. Surface and Coatings Technology, 2014, 259: 244−251.
[35] XU G, LUO A A, CHEN Y Q, SACHDEV A K. Interfacial phenomena in magnesium/aluminum bi-metallic castings [J]. Materials Science and Engineering A, 2014, 595: 154−158.
[36] ZHANG Qin-yun, ZHUANG Hong-shou. Brazing and soldering manual [M]. 2nd ed. Beijing: China Machine Press, 2008: 121−122. (in Chinese)

Al/Cu 双金属复合材料在液固复合铸造过程中的组织和性能

胡 媛，陈翌庆，李 立，胡焕冬，朱子昂

合肥工业大学 材料科学与工程学院，合肥 230009

摘 要：采用化学镀法在纯铜基体上镀上镍−磷镀层，并通过液固复合铸造工艺制备 Al/Cu 双金属材料。研究不同工艺参数(结合温度、预热时间)下 Al/Cu 接头的显微组织、力学性能和导电性能。结果表明，各种金属间化合物在界面处形成，其厚度和种类随结合温度和预热时间的增加而增加。Ni−P 夹层发挥了扩散阻碍层和保护膜的作用，有效地减少了金属间化合物的形成。Al/Cu 双金属复合材料的剪切强度和电导率随金属间化合物厚度的增加而减小，特别地，Al_2Cu 相的不利影响相比其他金属间化合物更加明显。在 780 °C 预热 150 s 条件下制备的试样表现出最大的剪切强度和电导率，其值分别为 49.8 MPa 和 5.29×10^5 S/cm。

关键词：Al/Cu 双金属；液固复合铸造；化学镀镍；Al_2Cu 相；显微组织；力学性能；电导率

(Edited by Wei-ping CHEN)